International Journal of Fluid Power 2 (2001) No. 3 pp. 23-31

REDUCTION OF QUASI-IMPULSIVE FORCES AND NOISE EMISSION IN THREE-SCREW PUMP ROTORS

Paolo Pennacchi[1], Giovanni Mimmi[2] and Lucia Frosini[2]

[1]*Politecnico di Milano, Dipartimento di Meccanica, Via La Masa 34, I-20158. Milano, Italy*
[2]*Università degli studi di Pavia, Dipartimento di Meccanica Strutturale, Via Ferrata 1, I-27100 Pavia, Italy*
paolo.pennacchi@polimi.it, mimmi@unipv.it, lucia@unipv.it

Abstract

In this paper a theoretical study is presented about the possibility of reducing the quasi-impulsive load components, which act on the rotors of the three-screw pumps in the rotational axial direction. These forces can be related, on the basis of previous experimental and analytical studies by the same authors, to the noise emission of the pump.

The analysis is carried out by the systematic variation of one of the design parameters of the rotors, i.e. the semi-amplitude of the threaded zone of the screws, by using the analytical tools previously set-up for the study of the dynamic loads on the standard rotors.

Finally, it is shown that a suitable choice of this design parameter on one hand allows to cancel the quasi-impulsive load, on the other hand has a positive effect on the loads on the cross section.

Keywords: three-screw pumps, noise reduction, rotor design, optimisation

This manuscript was received on 24 April 2001 and was accepted after revision for publication on 3 September 2001

1 Introduction

The starting points of this paper derive from previous studies of the same authors, in which they have developed an analytical model of three-screw pump rotors for the calculation of the dynamic loads (Mimmi and Pennacchi, 1998c). Along with these studies, experimental tests have been carried out in order to find the noise sources in these pumps (Mimmi et al, 1997) and devices for the noise emission reduction have been set-up (Mimmi and Pennacchi, 1998a). The noise emission reduction is a very important task for this type of pumps. In fact, among the different uses of the three-screw pump, that range from petrochemical industry to oleodynamic devices, an important application is the use as power unit for lifts in civil buildings. For this application it is important a particularly regular flow rate, which is an intrinsic characteristic of three-screw pumps, and a low level of noise emission.

In order to better understand the aims that have led to this study, it is useful to briefly resume the results obtained up to this time.

The analytical model, evaluated on the basis of standard design parameters (Mimmi and Pennacchi, 1998d), has shown an interesting behaviour of satellite screws that present quasi-impulsive twice per revolution dynamic loads in the rotation axis direction. In the plane normal to the rotation axis the dynamic load variation is periodic and limited in a specified angular range, which is almost corresponding with the wear zone that is find out in the pump housing after a certain operating life.

The studies on the noise emitted, which were carried out by means of the sound intensity technique (Mimmi et al, 1997; Mimmi and Pennacchi, 1998a), have shown that the main source of the noise can be located in the exhaust port and that the noise spectrum presents strong peaks in correspondence with the same harmonic components of the quasi–impulsive loads along the rotation axis. The modification proposed, and subsequently experimentally tested in Mimmi and Pennacchi (1998a), which consists of bypass channels between the chambers where the working fluid is transported and the delivery, are altogether effective for the noise emission reduction. However the frequency analysis shows that these devices are not likewise effective at the frequencies of the quasi-impulsive loads and at their superior harmonics, as expected by the developed theory.

The analytical tools employed here are the same used for the analytical model of the dynamic loads in

(Mimmi and Pennacchi, 1998c, 1998d) and briefly summarized in the following. The present theoretical study takes into account the possibility of reducing, or completely cancelling, the quasi-impulsive loads by optimising the design parameters.

The three-screw rotor design follows traditional rules that determine the ratios between inner and outer radiuses and the pitch radius. Among all the possible design parameters, whose minimum number determination is based on the study of the rotor geometry (Mimmi and Pennacchi, 1995), it has been chosen to vary the angle γ, which represents, on the cross section, the semi-amplitude of the worm of the central screw and therefore of the vane of the satellite screw (Fig. 1). In fact, a modification of the worm height, which could have interesting effects on the volumetric efficiency (Mimmi and Pennacchi, 1995), conflicts with the tradition rules and can weaken the satellite screw. Moreover a modification of the further design parameter, i.e. the helical pitch, has influence on the loads amplitude only (Mimmi and Pennacchi, 1998c), besides the flow rate, but not on their quasi-impulsive behaviour. Finally the helical lead angle is not an independent parameter, since it is function of the axial pitch and the pitch radius. The number of pitches, anyhow greater than a minimum value, that determines the length of the screw is not influent since for the loads determination it is sufficient to consider the last pitch towards the exhaust only (Mimmi and Pennacchi, 1998c).

The paper is organised as follows. In section 2 the results of a sound intensity measurements campaign are shown, in order to highlight the frequencies at which the noise emission is due to mechanical rather than fluid action. In section 3 the analytical model employed for the determination of the dynamics of the pressure loads on the pump rotors is briefly resumed and the expression for the calculation of the force is given. The results of the simulation are shown in section 4, where the twice per revolution components of the dynamic load are correlated to the harmonic components in the noise spectrum. Finally, in section 5 the possibility of reducing the dynamic load and the noise emission by varying the rotor geometry is illustrated.

2 Sound Intensity Measurements

In order to accurately analyse the characteristics of the noise emitted and possibly correlate the quasi-impulsive forces to the noise emission, a sound intensity measurements campaign has been carried out. In particular, the amplitude and frequency of the harmonic components along the body of the machine have been considered (Mimmi et al, 1997; Mimmi and Pennacchi, 1998a).

The set-up of traditional measurement techniques for the noise emission would have required a specific test rig in an anechoic chamber, to eliminate the sound emitted by the motor which drives the pump. This determines evident high costs and delays. The use of the intensity technique instead permits to avoid those problems (Fahy, 1989; Norton, 1989 and Mattia, 1990), by making the measurements directly on the field of the actual test circuit set-up in an industrial plant. In this case, it is not required to stop the other production cycles, and the sound power emitted by the pump in various working conditions can be satisfactorily distinguished from that of the motor.

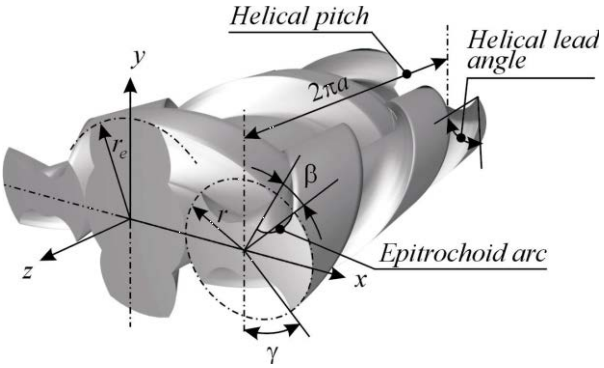

Fig. 1: *Central and satellite screws*

The sound intensity measurement procedures are described by ISO 9614-1 (1993) standard for the measurement at discrete points. In the case under exam this standard has been followed and besides other suggestions given in literature have been considered to obtain correct results (Jacobsen, 1994; Shirahatti and Crocker, 1994 and Schomer, 1996). The positioning of the sound intensity probe on the reference grid has been made manually. However it is possible to use automatic positioning by special devices and greater costs (Cervera et al, 1994 and Ravina, 1996).

The pump examined, was characterised by a flow rate of 0.005 m^3/s and is driven by a three-phase electric asynchronous motor with an operating velocity of 2950 rpm and a power of 18.5 kW.

The pressure stage of the pump was fixed at the values 0-2-4 MPa. The atmospheric pressure and the temperature, which are to be considered for the measurement and the calculations, were also measured during the testing session.

The instrumentation used for the sound intensity measurements was composed of: a sound intensity analyser Larson & Davis 2900, first used as sound-level meter for the measurement of the noise of the environment and then as intensity meter for the following direct measurements on the examined mechanical components; a sound intensity probe L & D 2250, made by two 1/2″ 'face-to-face' (*p-p*) microphones, with a separation distance of 12 mm; this separation value gives sufficient precision up to 5 kHz.

The probe has been calibrated (IEC 61043-1993 and IEC 60942-1997 standards) before the measurement session, since the most common error cause in this kind of measurement is the channel phase difference between the two microphones of the probe, as reported in literature (Fahy, 1989; Jacobsen, 1994; Jacobsen and Olson, 1994; Jarvis, 1994) and where the influence of air flows close to the probe on the measurement errors is stressed too. So the probe was shielded by a porous foam windscreen.

For the measurements, a discrete point method with a grid of 10×10 cm on four sides has been used (see Fig. 2), since two sides are shielded by metal plates which are the base and the pump support respectively. A thicker grid, of the type sometimes referred to in literature (Yokoi and Nakai, 1994), has not been used due to the pump dimensions and to the necessity of using a porous foam windscreen.

Therefore, 45 measurements have been made on the surface which encloses the pump, with an integrating time of 10 s each.

The acoustical analysis of the driving motor has been done by 59 measurements on a similar grid at the beginning of the measurement session.

The test rig was positioned inside a large shed, with an optimum disposition for all the sides except for the left that was adjacent to a wall.

As is well-known, the sound intensity vector $\boldsymbol{I}$ has the following definition:

$$\boldsymbol{I} = \frac{1}{T}\int_0^T p(\boldsymbol{x},t)\cdot \boldsymbol{v}(\boldsymbol{x},t)dt \qquad (1)$$

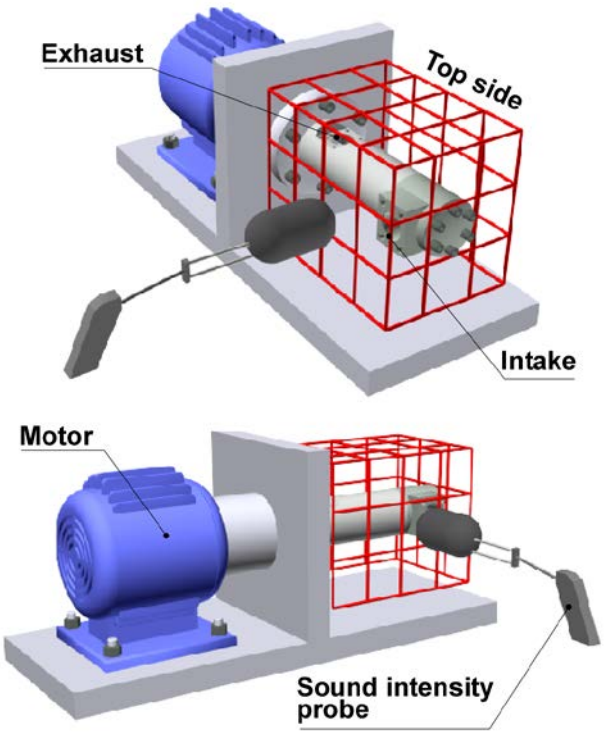

Fig. 2: *Scheme of the measuring grid*

Since it is hard to evaluate the velocity $\boldsymbol{v}(\boldsymbol{x}, t)$ at the measurement point, the *p-p* probes, which is adopted here, use Euler's equation for the determination of the velocity on the basis of the pressure gradient and reduce the latter to a finite difference (Norton, 1989). In practice, along the direction normal to the measurement surface, the sound intensity I_n is measured as:

$$I_n = -\frac{1}{\rho_0 \cdot \Delta x \cdot T}\int_0^T \left[\frac{p_1 + p_2}{2}\int_0^t (p_2 - p_1)\, d\tau\right] dt \qquad (2)$$

The integration of all the sound intensity data, measured at all the points of the grid which is the wrapping surface of the noise source, allows to obtain the sound power emitted by the pump or by the electric motor in the different configurations:

$$\Pi = \int_S I_n\, ds \qquad (3)$$

The sound power levels have been measured and the sound intensity maps for all sides and measurement configurations have been traced. A meaningful sample of one of these is shown in Fig. 3.

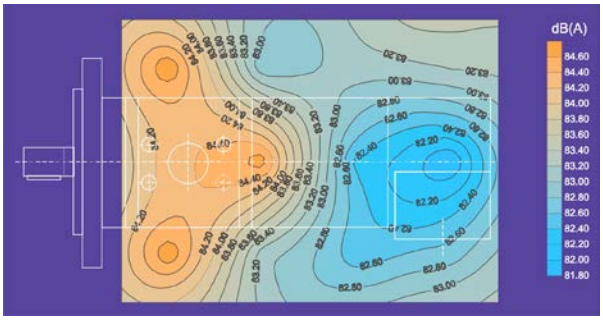

Fig. 3: *Sound intensity I_n map for the top side of a 0.005 m^3/s pump at 4 MPa, A-weighted*

As expected and as reported in Table 1, the sound power level emitted by the screw pump increases as the pump pressure stage increases.

Table 1: *Sound power levels*

Pressure stage [MPa]	Sound power Π level [dB(A)$_W$]
0	74.5
2	75.7
4	77.8

The sound intensity maps, which has been obtained by interpolation of the measured values of the sound intensity on the measuring grid, show some zones with relevant noise emission: on the top side a peak is present for all three of the pressure gaps (see Fig. 4). The exhaust port of the pumped fluid is positioned in that zone. The maps of the measurements carried out on the right and the front side of the pump show a noise concentration at the intake port. So we can infer that the most important noise sources of three-screw pumps are mainly the intake and the exhaust zones.

The analysis should not stop to the levels, but have to consider also the noise spectrum. Figure 4 shows a 1/3 octave band noise spectrum obtained, in which peaks appears on 100, 200…Hz. In order to better explain those peaks, the rich content of frequency which has been measured, and to possibly distinguish the noise sources, a theoretical model for the determination of the dynamics of the pressure loads on the pump rotors has been proposed by the authors (Mimmi and Pennacchi, 1997a, 1998c, 1998d) and is briefly resumed in the following section. This can help us to identify at which frequencies the noise emission is mainly due to mechanical rather than fluid actions.

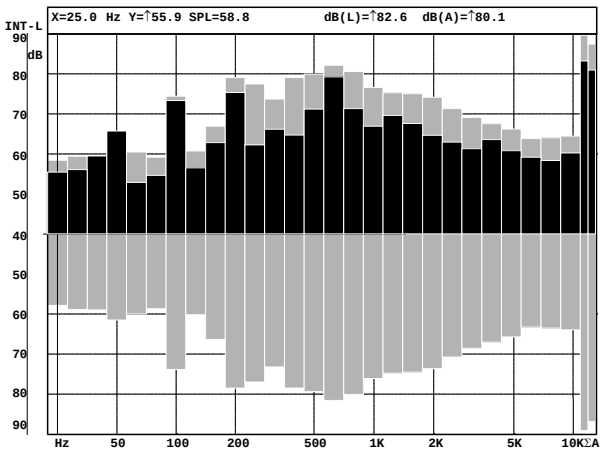

Fig. 4: *Noise spectrum*

3 The Analytical Model

In this section the analytical model employed is briefly resumed. This consists of two parts: first the analytical model of the rotor is obtained as shown also in Mimmi and Pennacchi (1998c). Then the loads acting during the rotation are calculated, following Adams and Soedel (1994, 1995).

An analytical model of the rotors is defined by means of the surfaces in the space[3] that compose it and that define several helicoids. Those surfaces, Fig. 5, are defined by the general equation in parametric form $P = P(u, \vartheta)$. Besides each surface, i.e. each flank of the screw, can be described by a vector $\boldsymbol{R}_i$ in the space[3]:

$$\boldsymbol{R}_i(u,\varphi,\vartheta) = \boldsymbol{B}(u)\,\boldsymbol{A}(\varphi)\,\boldsymbol{r}_i(\vartheta) \tag{4}$$

where $\boldsymbol{r}_i(\vartheta)$ is the vector in the plane xy which parametrically expresses one of the lines that form the cross section, i.e. the profile of the screw. For instance one of the epitrochoid arc of a satellite screw can be represented by:

$$\boldsymbol{r}_1(\vartheta) = \begin{bmatrix} 2\,r\cos(\vartheta-\gamma+\beta) - r_e\cos(2\vartheta-\gamma+\beta) \\ -2\,r\cos(\vartheta-\gamma+\beta) + r_e\cos(2\vartheta-\gamma+\beta) \\ 0 \\ 1 \end{bmatrix} \tag{5}$$

where γ and β are the design parameters, see Fig. 1, and ϑ is one of the surface coordinates variable in a range that is function of γ and β.

The matrix $\boldsymbol{A}(\varphi)$ is the clockwise rotation matrix in the plane xy of the complete helicoid and introduces the rotation of the screw along the z axis. If the central screw rotates counter clockwise, both satellite screws rotate clockwise.

$$\mathbf{A}(\varphi) = \begin{bmatrix} \cos(-\varphi) & -\sin(-\varphi) & 0 & 0 \\ \sin(-\varphi) & \cos(-\varphi) & 0 & 0 \\ 0 & 0 & 1 & 0 \\ 0 & 0 & 0 & 1 \end{bmatrix} \tag{6}$$

In fact, by multiplying the vector $\boldsymbol{r}_1(\vartheta)$ by the matrix $\boldsymbol{A}(\varphi)$ the arc given by Eq. 5 is rotated to $-\varphi$ and we obtain the vector which describes the arc in the plane[2]. This transformation is necessary because the sectors of surface, which are used for the calculation of the dynamic loads, vary as functions of rotor rotation angle φ.

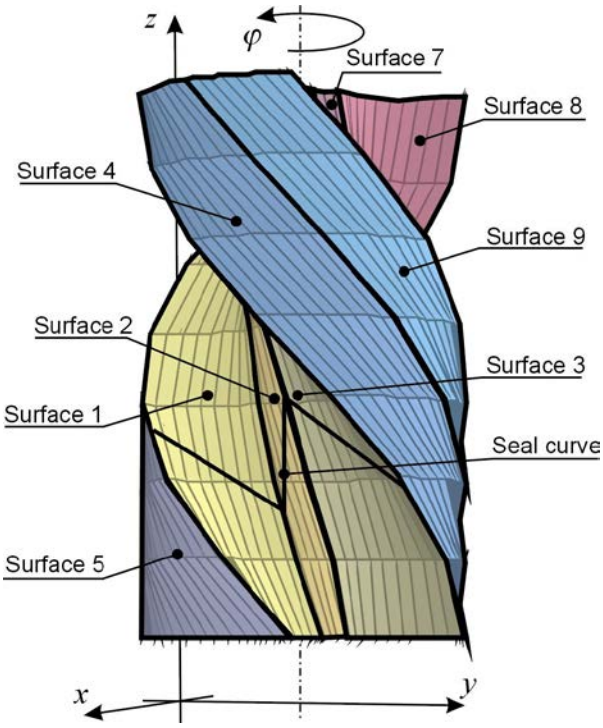

Fig. 5: *Helicoids that compose the rotor surface*

The matrix $\boldsymbol{B}(u)$ is the screw motion matrix that envelopes the rotor surface from its section and has the following expression, by considering left-handed screws and the fixed reference system with the origin on the central screw rotation axis:

$$\mathbf{B}(u) = \begin{bmatrix} \cos(-u) & -\sin(-u) & 0 & \pm 2r \\ \sin(-u) & \cos(-u) & 0 & 0 \\ 0 & 0 & 1 & a\,u \\ 0 & 0 & 0 & 1 \end{bmatrix} \tag{7}$$

where u is the second surface coordinate variable in the range $[0, 2\pi]$.

The screw flank is therefore obtained by multiplying the vector $\boldsymbol{A}(\varphi)\boldsymbol{r}_1(\vartheta)$, which is its base rotated in the plane xy of φ, by the matrix $\boldsymbol{B}(u)$. The resulting vector $\boldsymbol{R}_1$ describes the considered flank in the space[3].

Once the helicoids that compose the rotor surface are defined, it is necessary to determine the chambers, see Fig. 6, occupied by the fluid under pressure towards the exhaust. This is possible by defining the contact lines, i.e. the seal curves, between the satellite and the central screw as shown in Fig. 5 and analytically Mimmi and Pennacchi (1998c).

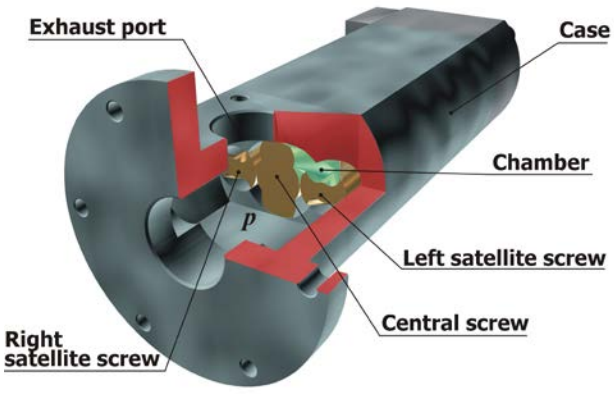

Fig. 6: *Chambers between the rotors*

Then it is possible to evaluate the dynamic loads by means of the method proposed in Mimmi and Pennacchi (1998c) and Adams and Soedel (1994, 1995) under some hypotheses of regularity for the surface P, which are generally satisfied in this case, and for a given value of pressure p. In the case examined, the force only, and not the moment, is considered.

Finally, it is possible to define the sector of surface S on the flanks of the rotors, see Fig. 7, where the working pressure p acts. Let dS be the area of a general infinitesimal element in the neighbourhood of a general point $Q(x, y, z)$ of the surface sector S expressed in parametric form as function of u and ϑ. The force $d\boldsymbol{F}$ on the infinitesimal element dS can be calculated as follows:

$$d\boldsymbol{F} = p\boldsymbol{n}\, dS \tag{8}$$

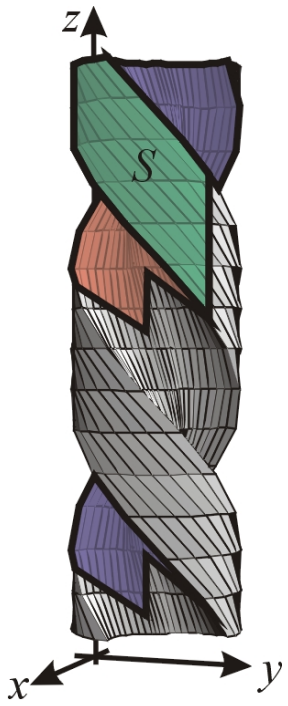

Fig. 7: *The surfaces on the satellite screw where the pressure act are darkened*

Since all the helical surfaces used for the modelling of the rotors are regular, the resulting force $\boldsymbol{F}$ can be calculated by means of surface integral:

$$\boldsymbol{F} = p\int_S \boldsymbol{n}\, dS = p\int_A \boldsymbol{n}\left|\boldsymbol{P}_u \times \boldsymbol{P}_\vartheta\right| dA =$$

$$= p\int_A \frac{\boldsymbol{P}_u \times \boldsymbol{P}_\vartheta}{\left|\boldsymbol{P}_u \times \boldsymbol{P}_\vartheta\right|}\left|\boldsymbol{P}_u \times \boldsymbol{P}_\vartheta\right| dA = p\int_A \boldsymbol{P}_u \times \boldsymbol{P}_\vartheta\, dA \tag{9}$$

where A is the domain of the surface parameters u and ϑ, which is function of φ, since the sectors of surface change with the angular position and P_u and P_ϑ are the partial derivative respect surface parameters u, ϑ of the parametric expression of the surfaces representing the rotor. Moreover the sectors of surface are made by different sub-sectors of surface on the different flanks, so the loads are eventually obtained by the sum (10) extended to all the flanks of the screw:

$$\boldsymbol{F}(\varphi) = p\left[\sum_i \int_{A_i(\varphi)} \boldsymbol{P}_u \times \boldsymbol{P}_\vartheta\, dA_i(\varphi)\right] \tag{10}$$

Equation 10 is then decomposed in its components F_x and F_y in the plane normal to the rotation axis and F_z along the same axis. The calculation is not trivial since it is necessary to consider the variation of the integration domain due to the rotation of the screw rotors.

4 Dynamic Load Simulation

The simulation of the dynamic behaviour of the satellite screw has been done in a case characterised by 1 MPa working pressure and by the following geometrical parameters: outer radius of the central screw r_e = 22.5 mm, pitch radius r = 13.5 mm and pitch 90 mm. The angle of semi-amplitude γ ranges between 34° to 47°.

First of all, let's analyse the component along z axis, by considering Fig. 8 and Fig. 9 that show F_z as function of both the rotor rotation angle φ and γ. In particular it can be observed in Fig. 8 that in correspondence of the value of γ equal to 34° or 47°, i.e. the extreme values of the considered range, the dynamic load has a constant and small value with superimposed a quasi-impulsive twice per revolution load. This main harmonic also clearly appears in the frequency analysis of F_z shown in Mimmi and Pennacchi (1998d).

In Fig. 9 a close-up particular of a 3D diagram is shown, close to the first of the two values of the rotation angles corresponding with the quasi-impulsive load.

By considering the behaviour in the plane xy, normal to the rotation axis, the diagrams of F_x and F_y do not show meaningful differences in the shape in the range from 34° to 47° from the diagram shown in Mimmi and Pennacchi (1998d) for γ equal to 45°. The component along x (Fig. 10) presents two jumps, in correspondence of φ equal to 90° and 270°, with a twice per revolution main harmonic component.

A similar behaviour, with a twice per revolution main harmonic component, is shown in Fig. 11 for the component along y.

These twice per revolution components of the dy-

namic load can be correlated to the strong peak at 100 Hz of the noise spectrum in Fig. 4. Since the motor has a revolving speed equal to 2950 rpm, the twice per revolution harmonic component has the frequency of about 100 Hz, while higher order harmonics have the frequencies of about 200 Hz, 300 Hz, etc.

By using this model, we can argue that the noise emission peaks of Fig. 4, corresponding to the indicated frequencies, are strictly related to the mechanical interaction between the rotors and the rotors and the case.

The other frequencies of the significant peak of noise emission can be attributed to the fluid action.

5 Reduction of Dynamic Load and Noise Emission

The presented simulated calculations of F_z (Fig. 8, Fig. 9) also show that, for γ values greater than 45°, which is the value commonly adopted, the angular amplitude, i.e., the range of φ in which the load in *z* direction has an high value, of the quasi-impulsive load has an increasing trend, while the amplitude is practically unchanged. The behaviour is different for values of γ less than 45°, in correspondence of which the angular amplitude of the quasi-impulsive load has a decreasing trend. The cancellation of the quasi-impulsive component along the *z* axis, in the case considered here, happens in correspondence of γ value equal to 37°, when the load is constant and small. For γ values less than 37° the quasi-impulsive load reappears in opposite direction.

By considering F_x (Fig. 10), we note that the amplitude of the twice per revolution components has a decreasing trend with the reduction of γ. In particular for $\gamma = 37°$, the jump amplitude is reduced of about 20% in respect to $\gamma = 45°$.

A similar result is obtained for F_y (Fig. 11), but in this case the reduction of the amplitude is of about 10%, when γ varies from 45° to 37°. It has been shown in Mimmi and Pennacchi (1998d) that the component of the dynamic loads in the plane *xy* are related to the wear produced by the screw rubbing on the housing, therefore the amplitude reduction of the components F_x and F_y will have a positive effect on reducing the wear too. The direction of the forces on the left satellite screw and their maximum and minimum values for $\gamma =$ 45° are reported in Fig. 12.

Finally the choice of a suitable value of γ allows to cancel the quasi-impulsive load along the rotation axis and reduces also the loads towards the housing. As a consequence of the correlation shown in the previous section of the quasi-impulsive component to the noise emission, it is right to expect a noise reduction, at least at the frequencies that have been eliminated. However the satellite screws, and obviously also the central, are different from the standard morphology (Fig. 13).

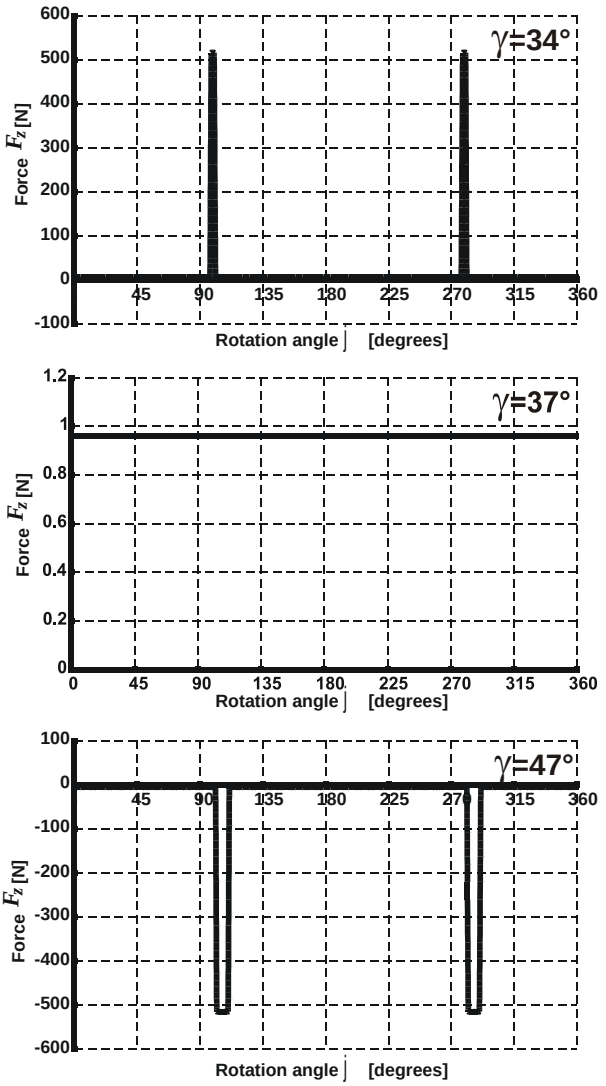

Fig. 8: *Dynamic load F_z along rotation axis as function of γ and rotation angle φ*

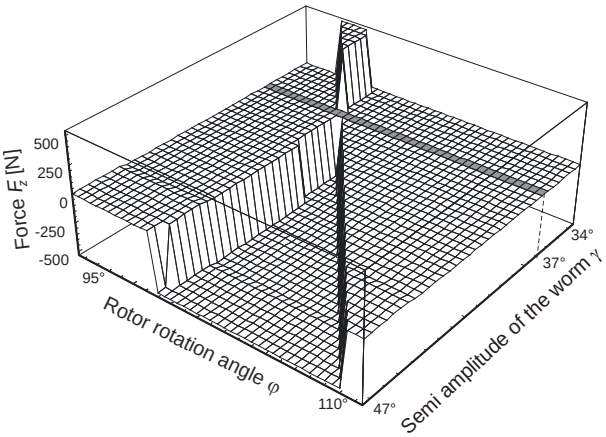

Fig. 9: *Dynamic load F_z along rotation axis as function of worm semi amplitude γ and of rotor rotation angle φ (detail)*

So the machining of these screws requires the use of special tools, whose design can be made following the methods reported f.i. in Litvin (1994), Mimmi and Pennacchi (1997b). Another disadvantage of the choice of a γ value less than the standard is the reduction of the section of the chambers. So if all the other design parameters are unchanged, the flow rate is reduced as follows from Mimmi and Pennacchi (1995).

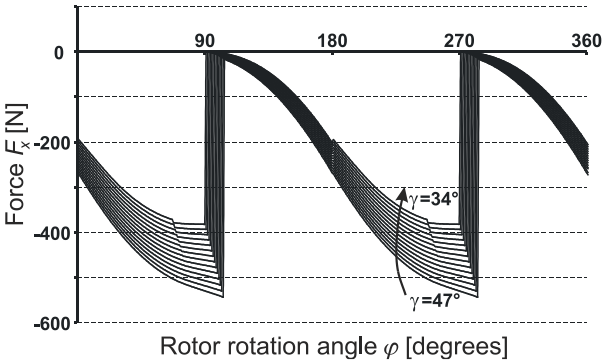

Fig. 10: *Dynamic load F_x along rotation axis as function of worm semi amplitude γ and of rotor rotation angle φ*

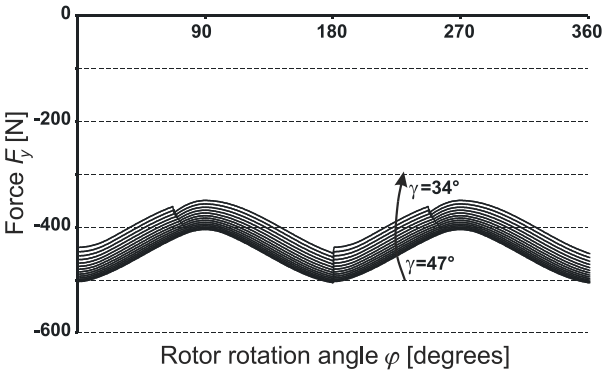

Fig. 11: *Dynamic load F_y along rotation axis as function of worm semi amplitude γ and of rotor rotation angle φ*

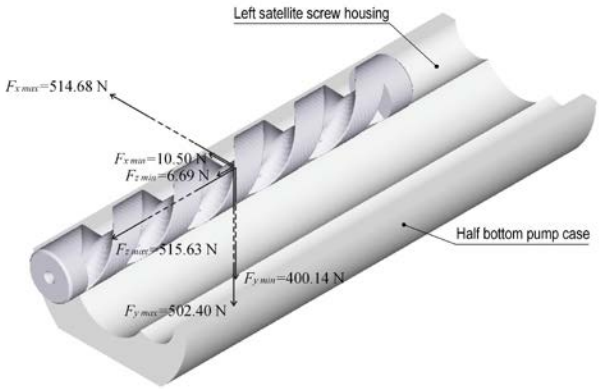

Fig. 12: *Direction of the forces on the left satellite screw and their maximum and minimum values for γ = 45°*

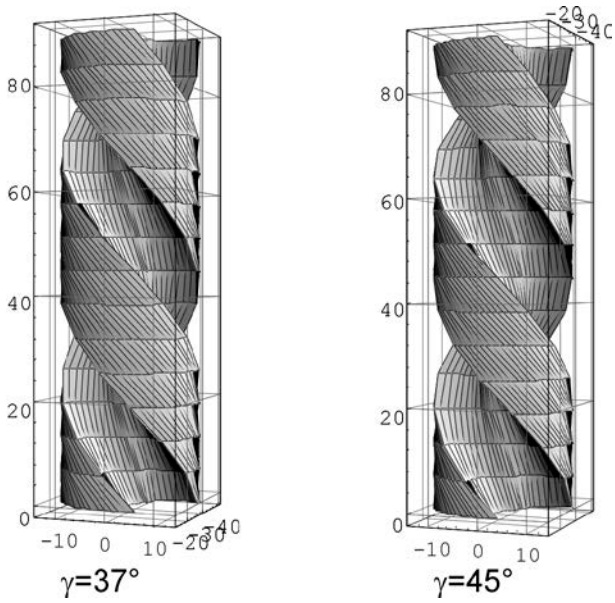

Fig. 13: *Comparison between modified (left) and standard rotor (right)*

6 Conclusion

In this paper a study is presented about the optimisation of the design parameters of the three-screw pump rotors in order to verify the possibility of cancel the quasi-impulsive dynamic load along the rotation axis of the screws. It is possible to show that the loads have components related to the peaks in the noise emission spectrum of the pump. It is verified that a suitable different choice of the semi-amplitude of the worm, usually equal to 45°, permits not only the cancellation of the quasi-impulsive component, but it is also effective in the reduction of the dynamic loads in the plane normal to the rotation axis.

Therefore it is possible to obtain positive effects reducing both the noise emitted and the wear of the housing. However some negative aspects are present, which are relative to the variation of this design parameter, such as the necessity of designing special machining tools and the reduction of the flow rate, being the others design parameters unchanged.

Nomenclature

$\mathbf{A}(\varphi)$	clockwise rotation matrix
A	surface coordinate domain
a	helix angular pitch
$\mathbf{B}(u)$	screw motion matrix
$\mathbf{F}$	force vector
F	force vector component
I	sound intensity vector
I_n	sound intensity along the direction normal to the measurement surface
$\mathbf{n}$	normal vector
P	surface function
p	working fluid operating pressure

R	surface vector
$\mathbf{r}$	line vector
r	rotor pitch radius, central rotor inner radius, idler rotor outer radius
r_e	central rotor outer radius
S	sector of surface
s	measurement surface
T	time period
t	measurement time
u	surface coordinate
$\mathbf{v}$	velocity at the measurement point
$\mathbf{x}$	measurement point
β	angle subtending an epicycloid or epitrochoid arc
Δx	distance between the two microphones
γ	semi-amplitude of the worm of the central screw in the cross section (semi-amplitude of not threaded zone of the screws)
φ	rotor rotation angle
Π	sound power
ρ_0	density
ϑ	surface coordinate

References

Adams, G. P. and **Soedel, W.** 1994. A method for computing the compression loads in twin screw compressors. *Proc. of 1994 International Compressor Engineering Conference at Purdue* (Ed W. Soedel), Purdue University, West Lafayette, Indiana, Vol. 1, pp. 67-72.

Adams, G. P. and **Soedel, W.** 1995. Computation of Compression Loads in Twin Screw Compressors. *ASME Journal of Mechanical Design*, Vol. 117, pp. 512-519.

Cervera, F., Belmar, F. and **Estellés, H.** 1994. A Low Cost Robot for Acoustic Intensity Measurements. *Noise Control Eng. Journal*, 42(1), pp. 31-35.

Fahy, F. J. 1989. *Sound Intensity*. Elsevier Science Publishers Ltd, London.

Jacobsen, F. 1994. Overview: The Current Status of Sound Intensity Measurements. *International Sound and Vibration Digest*, Vol. 1, No. 2, November 1994, Item 2.

Jacobsen, F. and **Olsen, E. S.** 1994. Testing Sound Intensity Probes in Interference Fields. *Acustica*, Vol. 80, No. 2, pp. 115-126**.**

Jarvis, D. R. 1994. The Calibration of Sound Intensity Instruments. *Acustica*, Vol. 80, No. 2, pp. 103-114.

Litvin, F. L. 1994. *Gear Geometry and Applied Theory*. Prentice-Hall, Englewood Cliffs, NJ.

Mattia, G. M. 1990. L'Intensimetria, Moderna Tecnica Diagnostica: Concetti Fondamentali di Teoria ed Applicazione delle Misure di Intensità Sonora. *Rivista Italiana di Acustica*, No. 4 Dicembre 1990, pp. LXXII-LXXXV (in italian).

Mimmi, G. and **Pennacchi, P.** 1995. Design of three-screw positive displacement rotary pumps. *Contact Mechanics II - Computational Techniques, M.H. Aliabadi and C. Alessandri eds.*, Computational Mechanics Publications, Southampton Boston, pp. 401-411.

Mimmi G. and **Pennacchi P.,** 1997a. "Carichi sui Rotori di Pompe a Viti Dovuti al Fluido in Pressione". *Proceedings of XIII Congresso Nazionale AIMETA*, Siena, 29 Sept. - 3 Oct. 1997, 2, pp. 7-12.

Mimmi, G. and **Pennacchi, P.** 1997b. Determination of Tool Profile for the Milling of Three Screw Pump Rotor. *Meccanica - International Journal of the Italian Association of Theoretical and Applied Mechanics*, Vol. 32, No. 4, pp. 363-376.

Mimmi, G., Pennacchi, P. and **Landoni, M.** 1997. Emissione sonora di una pompa a vite. *Oleodinamica e pneumatica*, No. 8, pp. 120-127 (in italian).

Mimmi, G. and **Pennacchi, P.** 1998a. Sound intensity technique applied to noise emission reduction. *Proc. of Mechanics in Design*, Nottingham, 6-9 July 1998.

Mimmi, G. and **Pennacchi, P.** 1998b. Reduction of quasi-impulsive forces in three-screw pump rotors. *Proc. of Theory an Practice of Gearing*, Izhevsk, Russia, 18-20 November 1998.

Mimmi, G. and **Pennacchi, P.** 1998c. Computation of rotor loads in three screw pumps. *ASME Journal on Mechanical Design*, Vol. 120, No. 4, December 1998, pp. 581-588.

Mimmi, G. and **Pennacchi, P.** 1998d. Dynamic effects of pressure loads in three screw pump rotors. *ASME Journal on Mechanical Design*, Vol. 120, No. 4, December 1998, pp. 589-592.

Norton, M. P. 1989. *Fundamentals of noise and vibration analysis for engineers*. Cambridge University Press.

Ravina, E. 1996. Analizzare l'Acustica delle Macchine con la Pneumatica. *Oleodinamica e pneumatica*, No. 3, marzo 1996, pp. 160-164 (in italian).

Schomer, P. D. 1996. 25 Years of Progress in Noise Standardization. *Noise Control Eng. Journal*, 44(3), pp. 141-148.

Shirahatti, U. S., Crocker, M. J. 1994. Studies on the Sound Power Estimation of a Noise Source using the Two-Microphone Sound Intensity Technique. *Acustica*, Vol. 80, No. 4, pp. 378-387.

Yokoi, M. and **Nakai, M.** 1994. Study of Portable Electric Drill Noise. *Noise Control Eng. Journal*, 42(4), pp. 129-136.

Paolo Pennacchi
Born on April 5th 1968, Milan (Italy). Degree, Ph.D. in Mechanics and Researcher at Politecnico di Milano, about 70 scientific publications on journals, congress and books. Participated to several MURST, ASI, CESI-ENEL, EDF, Brite EuRam "MODIAROT" research projects and to EU-India Economic Cross Cultural Program. His research fields are mainly rotordynamics, identification and diagnostics, kinematics, dynamics and design of mechanisms.

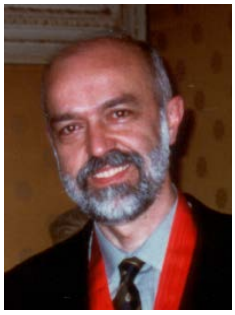

Giovanni Mimmi
Born on January 3rd 1947, Pavia (Italy). Full Professor of Applied Mechanics, more than 75 papers, on Journals, Congresses, books. Member of IFToMM Gearing & Transmissions TC, AAM, AIMETA, ASME, GIMC. Its researches has been supported by MURST, CNR, ASI, ENEL-CREL, Worthington, Pirelli Cavi, 3M Ferrania. Main research fields are kinematics, dynamics and design of mechanisms, identification and diagnostics, biomechanics.

Lucia Frosini
Born on May 4th 1970 in Pavia (Italy). Degree, Ph.D. in Electrical Engineering and post-doc contract at Università di Pavia. Author of about 20 scientific publications on journals and congress proceedings. Participated to MURST (Italian Ministry for University and Scientific Research) and ASI (Italian Space Agency) research projects. Her research fields are mainly identification and diagnostics applied to electrical machines and flexible manipulators.